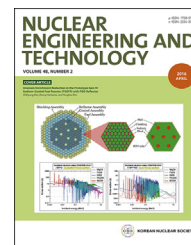


Available online at ScienceDirect

Nuclear Engineering and Technology

journal homepage: www.elsevier.com/locate/net

Original Article

Effect of Thermal Aging on Microstructure and Mechanical Properties of China Low-Activation Martensitic Steel at 550 °C

Wei Wang^{a,b}, Shaojun Liu^a, Gang Xu^{a,*}, Baoren Zhang^a, and Qunying Huang^a

^a Key Laboratory of Neutronics and Radiation Safety, Institute of Nuclear Energy Safety Technology, Chinese Academy of Sciences, No. 350, Shushanhu Road, Hefei, Anhui, 230031, China

^b University of Science and Technology of China, No. 96, Jinzhai Road, Hefei, Anhui, 230031, China

ARTICLE INFO

Article history:

Received 11 June 2015

Received in revised form

2 September 2015

Accepted 9 November 2015

Available online 12 December 2015

Keywords:

China Low-Activation Martensitic Steel

Ductile–Brittle Transition Temperature

Laves Phase

Thermal Aging

ABSTRACT

The thermal aging effects on mechanical properties and microstructures in China low-activation martensitic steel have been tested by aging at 550 °C for 2,000 hours, 4,000 hours, and 10,000 hours. The microstructure was analyzed by scanning and transmission electron microscopy. The results showed that the grain size and martensitic lath increased by about 4 μm and 0.3 μm, respectively, after thermal exposure at 550 °C for 10,000 hours. MX type particles such as TaC precipitated on the matrix and Laves-phase was found on the martensitic lath boundary and grain boundary on aged specimens. The mechanical properties were investigated with tensile and Charpy impact tests. Tensile properties were not seriously affected by aging. Neither yield strength nor ultimate tensile strength changed significantly. However, the ductile–brittle transition temperature of China low-activation martensitic steel increased by 46 °C after aging for 10,000 hours due to precipitation and grain coarsening.

Copyright © 2015, Published by Elsevier Korea LLC on behalf of Korean Nuclear Society. This is an open access article under the CC BY-NC-ND license (<http://creativecommons.org/licenses/by-nc-nd/4.0/>).

1. Introduction

The reduced activation ferritic/martensitic (RAFM) steels have been developed using modified (8–12)CrMoVNb type ferritic–martensitic steels by replacing Nb, Mo, and Ni with W, Mn, and Ta to obtain low activation capability [1]. RAFM steels are considered the primary candidate structural materials for future fusion power reactors because of their good thermo-physical properties, thermomechanical properties, and general industrial experience [2]. China low-activation

martensitic (CLAM) steel is a RAFM steel that was developed at the Institute of Nuclear Energy Safety Technology, Chinese Academy of Sciences, Hefei, China with the collaboration of many domestic and international institutes and universities [3–6]. It has been chosen as the primary structural material in the designs of FDS series PbLi blankets for fusion reactors, the China test blanket module for ITER (ITER CN TBM), and the breeder blanket of China fusion engineering test reactor [7]. A series of studies of CLAM steel have been done by the FDS team, including property measurement [8–12], welding

* Corresponding author.

E-mail address: gang.xu@fds.org.cn (G. Xu).
<http://dx.doi.org/10.1016/j.net.2015.11.004>

1738-5733/Copyright © 2015, Published by Elsevier Korea LLC on behalf of Korean Nuclear Society. This is an open access article under the CC BY-NC-ND license (<http://creativecommons.org/licenses/by-nc-nd/4.0/>).

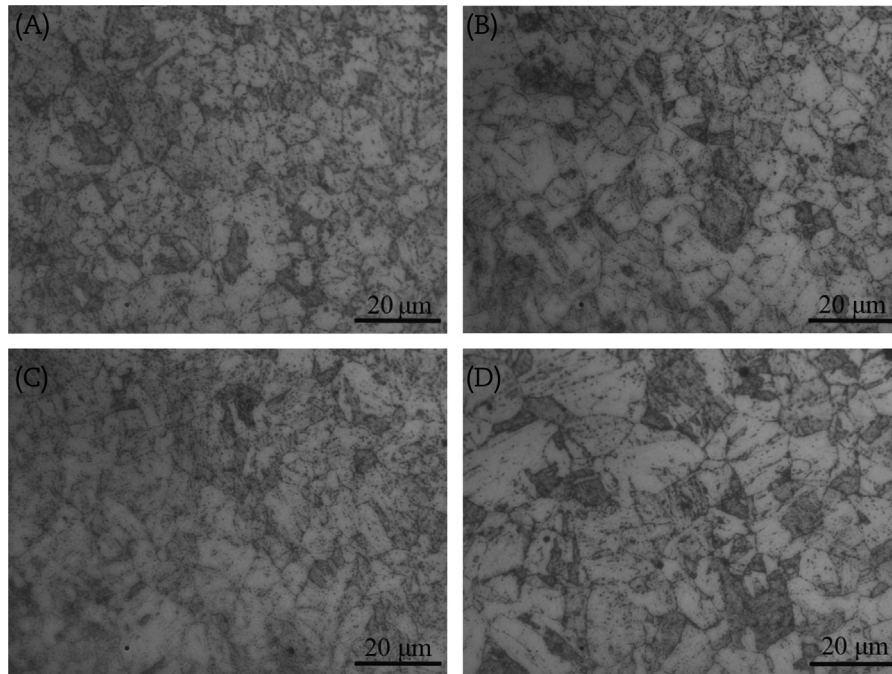


Fig. 1 – Optical micrographs of as-received and aged samples of China low-activation martensitic steel. (A) As-received; (B) 2,000 hours; (C) 4,000 hours; and (D) 10,000 hours.

techniques [13], post irradiation performance [14], and the research and development of TBM [15,16].

The upper limit temperature of the CLAM steel used in breeding blankets was proposed to be 550 °C. Hence, the thermal aging property is an important property to ensure the operation safety during exposure at the operating temperature. After long-term thermal exposure, the microstructure of RAFM steel will evolve, including precipitation and grain coarsening. This results in changes of mechanical properties. A number of thermal aging tests of other RAFM steels such as F82H and Eurofer have been conducted to characterize the microstructure evolution and properties change [17,18]. However, few studies were conducted on the aging effects of CLAM steel at 550 °C. The aim of the present work is to investigate the microstructure evolution and mechanical properties change of CLAM steel that has been aged at 550 °C up to 10,000 hours.

2. Materials and methods

The CLAM steel (HEAT 1005) used in this study was melted in a vacuum induction furnace and then electro-slag remelted into an ingot of 500 kg. The chemical composition of this material was 0.092% C, 8.9% Cr, 0.14% Ta, 0.15% V, 1.5% W, 0.05% Si, 0.49% Mn, 0.005% P, 0.002% S, and Fe in balance (in wt.%). The hot-rolled CLAM steel plate was heat treated with normalizing at 980 °C for 30 minutes and tempered at 760 °C for 90 minutes. Then, the tempered specimens were subjected to exposure at 550 °C for 2,000 hours, 4,000 hours, and 10,000 hours under air atmosphere in a tube furnace. The

machining allowance of each specimen was more than 2 mm to eliminate the oxidation effects on the mechanical properties of the specimens.

The microstructure of the aged specimens was analyzed with optical micrographs (OM), a scanning electron microscope (SEM), and a transmission electron microscope (TEM). The surfaces of all the specimens used in OM were etched with ferric chloride solution, and the OM was used to observe the grains of CLAM steel samples. The grain size was measured with microimage analysis and process software using linear intercept measurement. The samples for the SEM images were produced by electrolytic polishing. The electrolyte was a solution of 20% perchloric acid and 80% alcohol, and the operating voltage was 20 V. The Ø3 mm discs used for TEM observation were polished down to a thickness below 0.1 mm. Then the discs were electro-polished to their final thickness using a double jet electro-polisher with a solution of 10% perchloric acid and 90% alcohol at –8 °C.

The mechanical properties after aging were measured by tensile and Charpy impact tests. Both the cylindrical tensile samples (Ø5 mm) and the Charpy-V-notch samples (10 mm × 10 mm × 55 mm) were machined parallel to the rolling direction of the plates. The tensile tests for as-tempered and as-aged samples were conducted at a strain rate of 5×10^{-3} Hz in air at room temperature and 550 °C. Each condition for the tensile tests used three samples. The ductile–brittle transition temperature (DBTT) of CLAM was obtained by the Charpy impact test. The testing temperatures ranged from –120 °C to room temperature (RT), and there were not less than two samples for each condition of the Charpy impact tests.

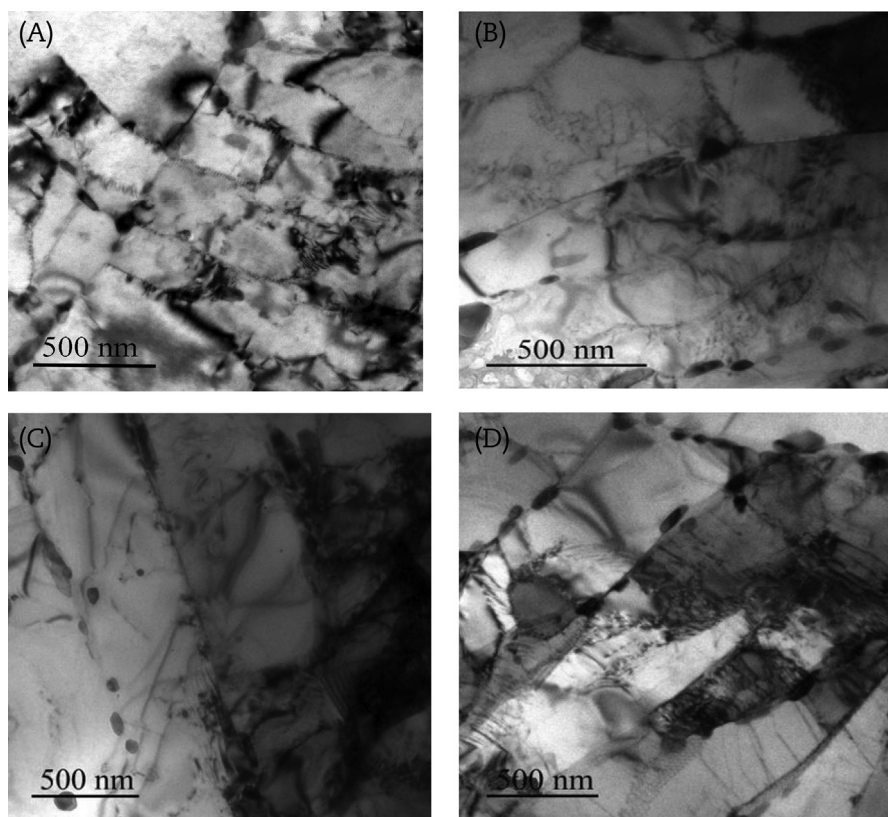


Fig. 2 – The transmission electron microscope images of aged samples of China low-activation martensitic steel. (A) As-received; (B) 2,000 hours; (C) 4,000 hours; and (D) 10,000 hours.

3. Results and discussion

3.1. Characterization of microstructure

The OM and TEM images of the as-received and aged samples are presented in Figs. 1 and 2, respectively, showing the microstructure evolution of the CLAM steel samples after long-term aging. No evident martensitic lath was found in the optical micrographs of any samples (Fig. 1). The reason may be that the martensitic lath was too thin to be observed with the OM. The average grain sizes of differently time-aged samples are presented in Table 1. Compared with the as-received sample the average grain size of the sample after aging for 10,000 hours was increased from 8.13 μm to 11.82 μm . The driving force of the migration of grain boundaries is surface energy. Hence, the grain coarsening is a spontaneous process during exposure at 550 $^{\circ}\text{C}$ for long time.

Table 1 – The average grain size of CLAM steel with different aging times.

Samples	Average grain size (μm)
As-received	8.13
2,000 hr	9.50
4,000 hr	10.02
10,000 hr	11.82

The martensitic lath boundary was observed clearly with TEM (Fig. 2). Fig. 2 shows that the tempered martensitic microstructure was relatively stable during aging at 550 $^{\circ}\text{C}$; the martensitic lath boundary could be observed clearly even after aging for 10,000 hours (Fig. 2D). Moreover, the most obvious evolution of the martensitic structure of CLAM sample was the lath coarsening for aging at 550 $^{\circ}\text{C}$. The width of the martensitic lath before aging (Fig. 2A) was $\sim 0.25 \mu\text{m}$, and it increased to $\sim 0.63 \mu\text{m}$ after aging for 10,000 hours (Fig. 2D). The prior austenite grain boundary (PAGB) and martensitic lath boundary are thermodynamically unstable structures. The boundaries would evolve gradually during the long-term aging at high temperature. Lath coarsening is the process of dislocation movement and annihilation. The increase of both temperature and time could augment the amount of dislocation movement and annihilation [19,20]. In this study, it was found that the lath boundaries were coarsened gradually with the increase of aging time, but the evolution of martensitic lath into subgrain was not significant, due to the lower aging temperature compared with other studies [21,22].

The precipitates played an important role in the microstructure stability for the heat-resistant steel during the long-term operation at high temperature. The SEM images of the as-received and aged samples of CLAM steel exhibited the evolution of size and distribution of precipitates (Fig. 3). The images show that the size of the M_{23}C_6 particles increased with increasing aging time. After aging for 10,000 hours, the

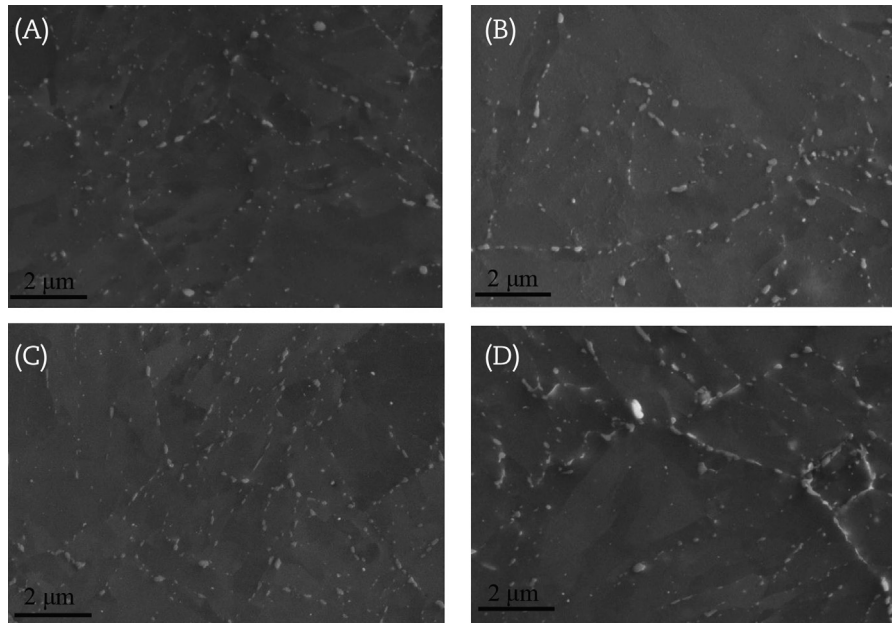


Fig. 3 – The scanning electron microscope images of as-received and aged samples of China low-activation martensitic steel. (A) As-received, (B) 2,000 hours, (C) 4,000 hours, and (D) 10,000 hours.

particles including $M_{23}C_6$ and Laves-phase are distributed unbrokenly in a network along the PAGB (Fig. 3D).

In as-received condition, the majority of precipitates were $M_{23}C_6$ type carbides and the other minorities were MX type particles. The $M_{23}C_6$ carbides basically precipitated along the PAGB and martensitic lath boundaries (Fig. 3A), and the morphologies of the $M_{23}C_6$ carbides presented as rod-shape, ellipsoid-shape, and spherical-shape. The chemical compositions of the $M_{23}C_6$ carbides were analyzed by Energy Dispersive Spectrometer (EDS) as shown in Fig. 4B. The result showed that the metal elements in the $M_{23}C_6$ carbides included Fe, W, and Cr, not only Fe and Cr. The reason could be that W partly replaced Cr in $(Fe,Cr)_{23}C_6$, then formed $(Fe,Cr,W)_{23}C_6$. After aging for 2,000 hours, the $M_{23}C_6$ carbides became larger and more evenly distributed than those of the as-received sample (Fig. 3B). The number of small size MX type carbides increased, and they mainly precipitated within martensitic laths (Fig. 4C). The EDS analysis of MX particles is shown in Fig. 4D. The results indicate that the MX type carbides were rich in Ta. According to other studies about RAFM steels [21,23], the Ta-rich particle might be TaC.

For longer aging (10,000 hours), a new kind of particle, which was mainly composed of Fe, W, and Cr, was formed in the CLAM steel. Tamura et al [23] identified that the new kind of W-rich particle as Laves-phase. Generally, Laves-phase was precipitated along the PAGB and martensitic lath boundaries, and it associated with $M_{23}C_6$ to reduce the phase transformation free energy, thereby raising the nucleation rate and reduce the critical nucleation energy [24]. The Laves-phase engulfed $M_{23}C_6$ carbides, especially the W-rich carbides, to consume the W element. The Laves-phase presented as the rod-shaped particles shown in Fig. 4G. The length and width of the Laves-phase was about 361 nm and 89 nm, respectively. The chemical composition of Laves-phase was 34Fe-9Cr-56W-Mn (in wt%) analyzed by the EDS (Fig. 4H).

3.2. Tensile properties

The results of ultimate tensile strength (R_m) and yield strength ($R_{p0.2}$) of CLAM steel before and after different aging times are shown in Fig. 5. The test temperatures were 550 °C and RT.

The strength of the CLAM steel was not changed obviously during the thermal exposure at 550 °C up to 10,000 hours. The ultimate tensile strength at RT was increased by 21 MPa after aging for 2,000 hours, and then the samples exhibited slight softening with the increasing of aging time. The same variation tendency was exhibited at 550 °C tensile testing. However, the yield strength at RT presented a different variation tendency compared with the ultimate tensile strength after long-term aging at 550 °C (Fig. 5). It slightly decreased after aging for 2,000 hours. The reason could be that the error of yield strength at RT was larger than the others as, shown in Fig. 5.

After aging for 2,000 hours, the TaC increased obviously. Generally, the dislocation movement could be pinned by second-phase particles, that induced precipitation strengthening, and led to a slight increase in strength. After aging over 4,000 hours, the formation of Laves-phase was at the expense of the dissolved W near the grain boundary and $M_{23}C_6$ carbides, which reduce the solid solution strengthening and counteract the increase of strength by TaC particles. The new Laves-phase nucleated at the boundary next to the $M_{23}C_6$ particles. So, the Laves-phase and $M_{23}C_6$ carbide were connected together as a single large particle. Hence, the Laves phase could not provide the precipitation strengthening by itself, which could lead to a slight decrease in strength after aging for more time.

3.3. Charpy impact properties

The upper shelf energy and DBTT of the CLAM steel sample after aging for different times were obtained by Charpy impact

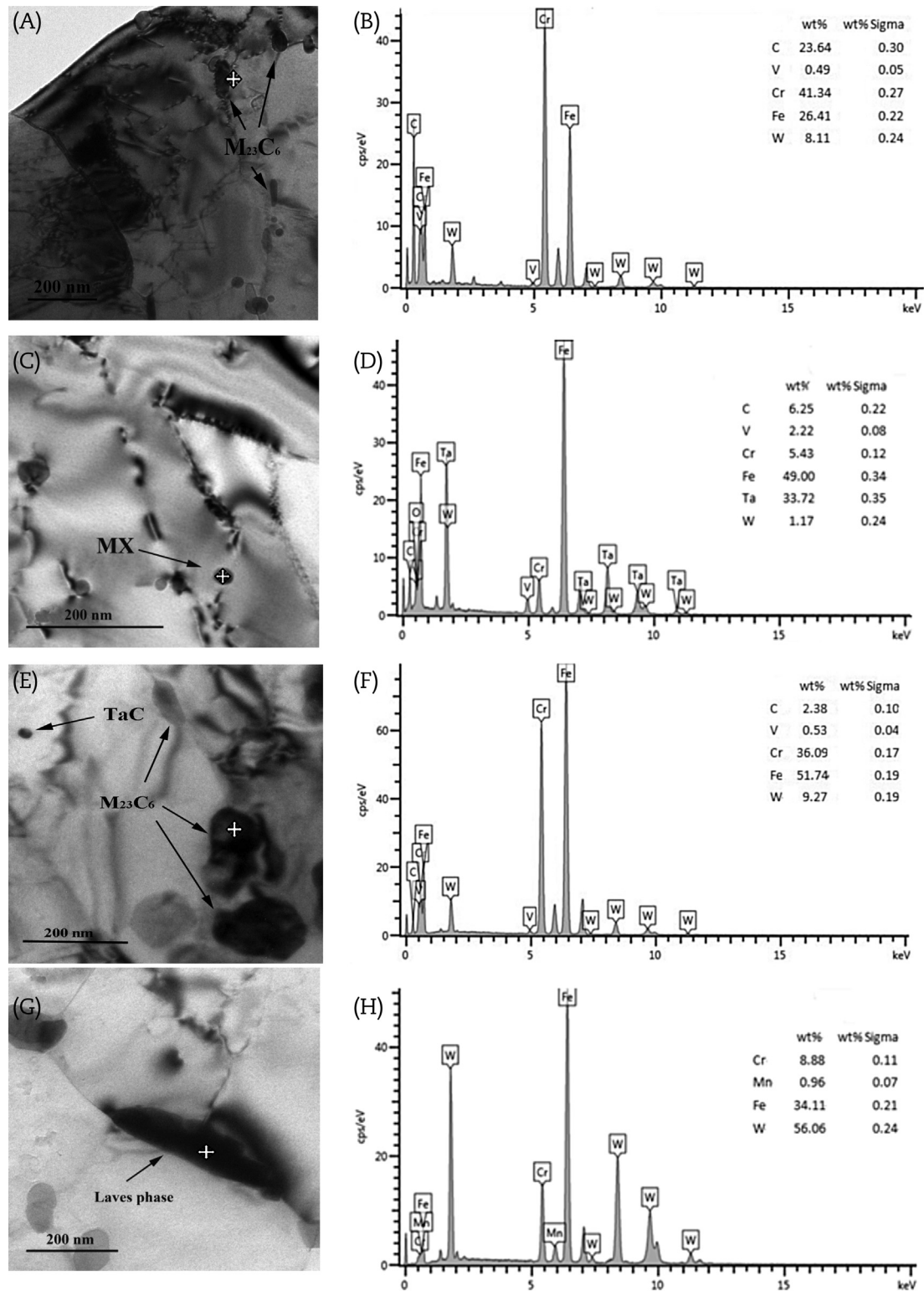


Fig. 4 – The transmission electron microscope images and EDS analysis of precipitates of as-received and aged samples of China low-activation martensitic steel. (A, B) as-received; (C, D) 2,000 hours; (E, F) 4,000 hours; and (G, H) 10,000 hours.

tests, and the results are presented in Fig. 6. The upper shelf energy of the samples changed slightly and the impact absorbing energy at RT only decreased by 7 J compared with that of the as-received condition even after aging for 10,000

hours. However, the DBTT of the thermally-aged CLAM steel increased remarkably by about 46 °C.

Many factors, including grain size and precipitates, could influence the DBTT. A small grain size provides a higher grain

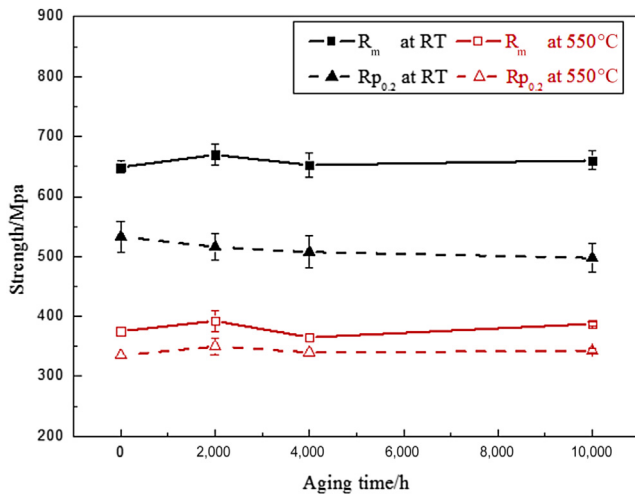


Fig. 5 – Strength of the China low-activation martensitic steel after long-term thermal aging.

boundary area per unit volume, which retards or deviates the propagation of cleavage cracks. Thus, it eventually leads to a toughness increase. However, only high-angle boundaries (HAB) such as prior austenite grain boundaries and martensitic packet boundaries are effective in retarding or deflecting the crack propagation [25]. The martensitic lath boundaries, which are low-angle boundaries, are ineffective in retarding the crack propagation for small boundary misorientation. The grain size of CLAM steel was increased by about 4 μm after aging at 550 $^{\circ}\text{C}$ for 10,000 hours as shown in Table 1, which could reduce the toughness and increase the DBTT of CLAM steel. The relationship between grain size and DBTT can be given by the following equation [26]:

$$\alpha \times \text{DBTT} = \beta - \ln(d_{\text{eff}})^{-1/2} \quad (1)$$

where α and β are constants, and d_{eff} is effective grain size. The equation indicates that the DBTT increases with the increase of effective grain size.

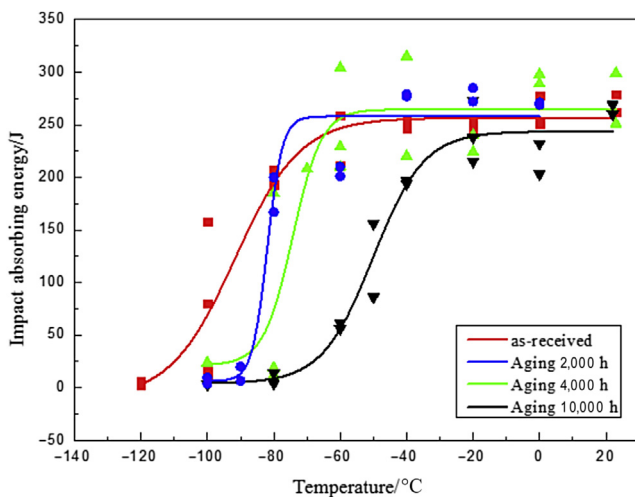


Fig. 6 – Impact curves of the China low-activation martensitic steel after long-term aging at 550 $^{\circ}\text{C}$.

Precipitates could play an important role in impact toughness. The nucleation of microvoids or initiation of cleavage cracks usually occur at the particle–matrix interface or the fracture of particles [27]. After aging for 10,000 hours, the size of M_{23}C_6 was increased, and new Laves-phase was formed and expanded. Cavities would nucleate at boundaries between the large particles and matrix. Particles with an average size > 0.13 μm could trigger the fracture mode transformation from transgranular fracture to intergranular fracture [21]. Hence, it was understandable that the DBTT was increased by 46 $^{\circ}\text{C}$ after aging for 10,000 hours.

The influence of thermal aging on the microstructure and the mechanical properties of CLAM steel were investigated in this study. The results are summarized as follows. (1) The martensitic lath could be observed clearly with TEM. The sizes of grains and martensitic lath were increased by about 4 μm and 0.3 μm , respectively, after long-term exposure at 550 $^{\circ}\text{C}$ for 10,000 hours. (2) The Laves-phase was discovered in the samples after aging for 10,000 hours at 550 $^{\circ}\text{C}$. It was mainly nucleated at the grain boundaries to reduce the critical nucleation energy. (3) The strength of the CLAM steel was not obviously changed during the thermal exposure at 550 $^{\circ}\text{C}$ up to 10,000 hours. (4) The DBTT of the CLAM steel sample was increased by 46 $^{\circ}\text{C}$ after aging for 10,000 hours. This was caused by the grain coarsening and the particle precipitation.

Conflicts of interest

All authors have no conflicts of interest to declare.

Acknowledgments

This work was supported by the Special Foundation of the President of Hefei Institutes of Physical Science with Grant No. YZJJ201326, and the National Basic Research Program of China with Grant Nos. 2013GB108005 and 2014GB112003. The authors would like to thank Prof. Y.C. Wu for his guidance on this work, and show their great appreciation to the other members of the FDS Team for their support and contribution to this research.

REFERENCES

- [1] R. Lindau, A. Moslang, M. Rieth, M. Klimiankou, E. Materna-Morris, A. Alamo, A.A.F. Tavassoli, C. Cayron, A.M. Lancha, P. Fernandez, N. Baluc, R. Schäublin, E. Diegele, G. Filacchioni, J.W. Rensman, B.V.D. Schaaf, E. Lucon, W. Dietz, Present development status of EUROFER and ODS-EUROFER for application in blanket concepts, *Fusion Eng. Design* 75–79 (2005) 989–996.
- [2] Q. Huang, N. Baluc, Y. Dai, S. Jitsukawa, A. Kimura, J. Konys, R.J. Kurtz, R. Lindau, T. Muroga, G.R. Odette, B. Raj, R.E. Stoller, L. Tan, H. Tanigawa, A.A.F. Tavassoli, T. Yamamoto, F. Wan, Y. Wu, Recent progress of R&D activities on reduced activation ferritic/martensitic steels, *J. Nucl. Mater.* 442 (2013) S2–S8.
- [3] Q. Huang, C. Li, Y. Li, M. Chen, M. Zhang, L. Peng, Z. Zhu, Y. Song, S. Gao, Progress in development of China low

- activation martensitic steel for fusion application, *J. Nucl. Mater.* 367–370 (2007) 142–146.
- [4] Q. Huang, C. Li, Q. Wu, S. Liu, S. Gao, Z. Guo, Z. Yan, B. Huang, Y. Song, Z. Zhu, Y. Chen, X. Ling, Y. Wu, FDS Team, Progress in development of CLAM steel and fabrication of small TBM in China, *J. Nucl. Mater.* 417 (2011) 85–88.
- [5] Q. Huang, Y. Wu, J. Li, F.R. Wan, J.L. Chen, G.N. Luo, X. Liu, J.M. Chen, Z.Y. Xu, X.G. Zhou, X. Ju, Y.Y. Shan, J.N. Yu, S.Y. Zhu, P.Y. Zhang, J.F. Yang, X.J. Chen, S.M. Dong, Status and strategy of fusion materials development in China, *J. Nucl. Mater.* 386–388 (2009) 400–404.
- [6] Q. Huang, FDS Team, Development status of CLAM steel for fusion application, *J. Nucl. Mater.* 445 (2014) 649–654.
- [7] Q. Huang, Q. Wu, C. Li, S. Liu, B. Huang, Progress in development of Fabrication of small TBMs for EAST and ITER, *Fusion Eng. Design* 85 (2010) 2192–2195.
- [8] Y. Li, Q. Huang, Y. Wu, T. Nagasaka, T. Nagasaka, T. Muroga, Mechanical properties and microstructures of China low activation martensitic steel compared with JLF-1, *J. Nucl. Mater.* 367–370 (2007) 117–121.
- [9] Q. Huang, S. Gao, Z. Zhu, M. Zhang, Y. Song, C. Li, Y. Chen, X. Ling, X. Zhou, Progress in compatibility experiments on lithium-lead with candidate structural materials for fusion in China, *Fusion Eng. Design* 84 (2009) 242–246.
- [10] Y. Wu, Q. Huang, Z. Zhu, S. Gao, Y. Song, R&D of DRAGON series lithium lead loops for material and blanket technology testing, *Fusion Eng. Design* 62–1 (2012) 272–275.
- [11] Y. Li, T. Nagasaka, T. Muroga, Long-term thermal stability of reduced activation ferritic/martensitic steels as structural materials of fusion blanket, *Plasma Fusion Res.* 5 (2010) S1036–S1039.
- [12] S. Gao, Q. Huang, Z. Zhu, Z. Guo, X. Ling, Y. Chen, Corrosion behavior of CLAM steel in static and flowing LiPb at 480°C and 550°C, *Fusion Eng. Design* 86 (2011) 2627–2631.
- [13] C. Li, Q. Huang, Q. Wu, S. Liu, Y. Lei, T. Muroga, T. Nagasaka, J. Zhang, J. Li, Welding techniques development of CLAM steel for test blanket module, *Fusion Eng. Design* 84 (2009) 1184–1187.
- [14] Q. Huang, J. Li, Y. Chen, Study of irradiation effects in China low activation martensitic steel CLAM, *J. Nucl. Mater.* 329 (2004) 268–272.
- [15] Y. Wu, FDS Team, Conceptual design and testing strategy of a dual functional lithium-lead test blanket module in ITER and EAST, *Nucl. Fusion* 47–11 (2007) 1533–1539.
- [16] Y. Wu, FDS Team, Design analysis of the china dual-functional lithium lead (DFLL) test blanket module in ITER, *Fusion Eng. Design* 82 (2007) 1893–1903.
- [17] H. Hadraba, I. Dlouhy, Effect of thermal ageing on the impact fracture behavior of Eurofer'97 Steel, *J. Nucl. Mater.* 386–388 (2009) 564–568.
- [18] K. Shiba, H. Tanigawa, T. Hirose, H. Sakasegawa, S. Jitsukawa, Long-term properties of reduced activation ferritic/martensitic steels for fusion reactor blanket system, *Fusion Eng. Design* 86 (2011) 2895–2899.
- [19] H. Cerjak, P. Hofer, B. Schaffernak, The influence of microstructural aspects on the service behavior of advanced power plant steel, *ISIJ Int.* 39 (1999) 874–888.
- [20] C. Panait, W. Bendick, A. Fuchsmann, A.F. Gourgues-Lorenzon, J. Besson, Study of the microstructure of the grade 91 steel after more than 100,000 h of creep exposure at 600°C, *Int. J. Pressure Vessels Piping* 87–6 (2010) 326–335.
- [21] X. Hu, L. Huang, W. Yan, W. Wang, W. Sha, Y. Shan, K. Yang, Evolution of microstructure and changes of mechanical properties of CLAM steel after long-term aging, *Mater. Sci. Eng. A* 586 (2013) 253–258.
- [22] F. Abe, S. Nakazawa, H. Araki, T. Noda, The role of microstructural instability on creep behavior of a martensitic 9Cr-2W steel, *Metallurgical Trans. A* 23 (1992) 469–477.
- [23] M. Tamura, K. Shinozuka, H. Esaka, S. Sugimoto, K. Ishizawa, K. Masamura, Mechanical properties of 8Cr-2WVTa Steel Aged for 30000 h, *J. Nucl. Mater.* 283–287 (2000) 667–671.
- [24] G. Hu, X. Cai, Y. Rong, *Foundation of Materials Science*, second ed., Shanghai Jiao Tong University Press, Shanghai, 2006.
- [25] A. Chatterjee, D. Chakrabarti, A. Mitra, R. Mitra, A.K. Bhaduri, Effect of normalization temperature on ductile-brittle transition temperature of a modified 9Cr-1Mo steel, *Mater. Sci. Eng. A* 618 (2014) 219–231.
- [26] M. Zhao, T. Zeng, J. Li, H. Xiaofang, Y.C. Zhao, A. Atrens, Identification of the effective grain size responsible for the ductile to brittle transition temperature for steel with an ultrafine grain size ferrite/cementite microstructure with a bimodal ferrite grain size distribution, *Mater. Sci. Eng. A* 528 (2011) 4217–4221.
- [27] A. Ghosh, A. Ray, D. Chakrabarti, C.L. Davis, Cleavage initiation in steel: competition between large grains and large particles, *Mater. Sci. Eng. A* 561 (2013) 126–135.